Proceedings of the
Third European Conference on Structural Control, 3ECSC,
12-15 July 2004, Vienna University of Technology, Vienna, Austria

ANALYTICAL MODEL FOR HIGH DAMPING ELASTOMERS APPLIED TO ENERGY DISSIPATING DEVICES. NUMERICAL STUDY AND EXPERIMENTAL VALIDATION

Pablo Mata[1], Ruben Boroschek[2], AlexBarbat[3], Sergio Oller[4]

[1] Technical University of Catalonia, Edificio C1, Campus Norte UPC
Gran Capitán s/n. Barcelona 08034, Spain
[2] Civil Engineering Department. University of Chile, Blanco Encalada 2002
Santiago, Chile

In this work the results of a study carried out to characterize the mechanical response of a high damping rubber to be used to design and construct energy dissipating devices and base isolators for controlling strong vibrations in civil engineering structures is presented. A new parametric model of the rubber is proposed to be employed in the design procedure and structural analysis of passive controlled structures. The parameters of the model are calibrated using experimental results obtained from tests on rubber specimens subjected to different loading paths. The response predicted by the proposed model is compared with these obtained from experimental tests.

Keywords: *Rubber, passive control, seismic*

1 Introduction

Rubber is one of the most frequently used materials in the construction of base isolator devices for controlling vibrations induced by earthquakes. Additionally, it has been proposes for energy dissipating devices. The mechanical characteristics of rubber depend strongly on the composition of the mixture used in the fabrication of the material. Refs. [1,3,4]. In general, its mechanical behavior is complex presenting an elastic modulus strongly dependent on the deformation level and loading frequency. Additionally, when the material undergoes large strains and depending on the boundary conditions, a noticeable hardening phenomenon appears in the strain-stress response. It is possible to find numerical models of the problem based on the principles of the solid continuous mechanics, but normally they requires a large amount of computer time and the convergence of the problem is not ensured.

Other kind of models can be obtained by means of fitting parametrical equations to the curves obtained experimentally, Ref. [4], providing a rule for the description of the material, and in many cases, of the control devices. This last option presents the advantage of being much more economic in computing time and it is possible to calibrate the model directly from loading tests carried out on the material or control devices.

Frequently, the practical design of structures with rubber based control systems uses equivalent linear models for the controlling devices. The use this kind of models can induce significant errors in the estimation of the energy dissipated by the devices due to that the model parameters are constants for all strain levels and loading frequency, Ref. [4].

This work propose a new analytical model for rubbers. The parameters of the model are determined from experimental tests. Finally, the response of the new model is compared with experimental data.

2 Mechanical characterization

This part of the work presents the test assembly and the results obtained from tests carried out to characterize the mechanical properties of a high damping rubber. The force–displacements response of the rubber was obtained for different loading paths which include sinusoidal cycles of imposed displacements with different amplitudes and frequencies and sequences of arbitrary imposed displacements. The dependency between dissipated energy and loading frequency or maximum strain level was studied.

[1] Pablo Mata, pmata@cimne.upc.es
[2] Rubén Boroschek, rborosch@ing.uchile.cl
[3] Alex Barbat, alex.barbat@upc.es
[4] Sergio Oller, sergio.oller@upc.es

2.1 Description of the experimental assembly and test program

Three specimens were constructed, each of them was composed by five segments, the both extreme segments and the central one was made of steel with circular perforations for providing the fixation to the test machine. The other two segments were constituted by rubber plates of 9 cm^2 of area and 6 mm of thickness. The faces of the rubber plates were adhered to the contiguous steel bodies. By this way, fixing the both extremes and forcing a displacement in the intermediate one it is possible to develop different loading paths of imposed displacements, Fig. 1. The sequence of loading tests was the following:

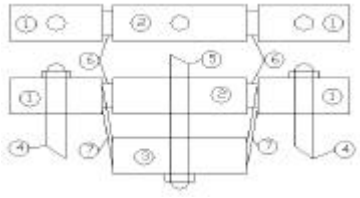

Figure 1: Specimen description. 1: Fixed steel segments. 2: Movable steel segment. 3: Position of the movable segment when a displacement is imposed on the specimen. 4: Fixating bolts. 5: Movable embolus. 6: Rubber plate in original configuration. 7: Deformed rubber specimen.

Symmetric sinusoidal cycles. The specimens were subjected to sinusoidal loading cycles of imposed displacements. The range of maximum applied amplitudes was defined by following values: +/- 10, 20 50, 100, 150, 170 and 200 %, carrying out each test with the following loading frequencies: 1/30, 0,5, 1,0 and 2,0 Hz.

Asymmetric sinusoidal cycles. Sinusoidal cycles of imposed displacement with different maximum and minimum amplitudes were applied. The test were carried out with a loading frequency of 0,5 Hz. See Table 1 for detailed values of maximum and minimum amplitudes. By means of this set of tests it has tried to characterize the hysteretic behavior of the rubber for loading cycles which are displaced from the origin.

Table 1: Asymmetric loading tests.

Test	1	2	3	4	5	6	7	8	9	10	11	12
max %	200	200	200	200	200	200	200	200	150	150	150	150
Min %	170	150	100	50	20	-20	-50	-100	100	50	20	-20
Test	15	16	17	18	19	20	21	22	23	24	25	26
max %	100	100	100	100	100	100	50	50	50	50	50	50
Min %	50	20	-20	-50	-100	-150	20	0	-20	-50	-100	-150

Arbitrary imposed displacements. Finally the specimens were subjected to sequences of arbitrary imposed displacements. The first one corresponds to a sequence of ascending and descending ramps. The second one is a scaled duplicate of the component N–S of the El Centro earthquake 1940.

2.2 General behavior of the rubber

The general behavior of the rubber shows a nonlinear strain–stress relationship with energy dissipation. When a test specimen is subjected by first time to sinusoidal cycles, a *progressive stiffness degradation* is noticeable. The degrading process progress until a stable hysteretic cycle is obtained. This progressive lack of stiffness could be explained as a transient process of rearrangement of the particles which composes the material. Ref. [5].

One of the main characteristics of the rubber is a strongly variable elastic modulus. From the symmetric loading tests is possible to identify three different zones:

An initial zone, for strains in the range +/-20 %. This zone is characterized by higher slope of the line tangent to the strain–stress curve than in the rest of the strain ranges. A *central zone* (2), contained in the range +/- [20–150] %, where the slope of the mentioned tangent line decrease. An *ending zone* (3), for strain levels higher than 150 % where hardening is present.

2.3 Dissipated energy.

In this work the dissipated energy was calculated estimating the area of the hysteretic cycle Ref. [2,4].

2.3.1 Dependency between the dissipated energy and the strain level.

The Fig. 2 on the right side shows the obtained values for the dissipated energy as function of the maximum strain level for different loading frequencies. The dissipated energy increases with the maximum strain level. However, the rate of energy dissipation is not constant due to that for low strain levels the cycles has an approximately elliptic shape, but as the strains grows the hysteretic cycles are stretched along the mayor axis of the ellipse.

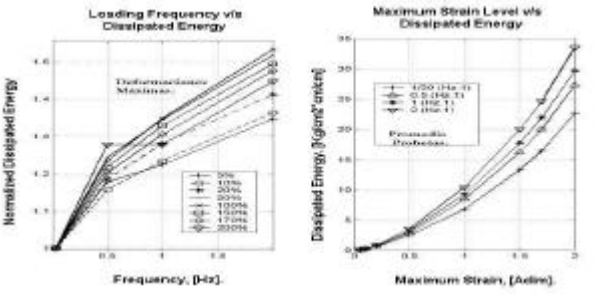

Figure 2: Left: Dependency between dissipated energy and loading frequency. Right: Dependency between dissipated energy and maximum strain level for each loading frequency.

2.3.2 Dependency between dissipated energy and loading frequency

In the Fig. 2 on the left side it is possible to see the dependency between dissipated energy and loading frequency. Dissipation increase with frequency indicating that viscous forces are present. The results depicted in this figure are normalized for the test carried

out at 1/33 Hz. The rate of dissipation is maintained constant for damping values higher than 0.5 Hz. In the first range of frequencies, (1/33–0.5 Hz), a higher slope of the curve is obtained independently of the strain level. A possible explanation for this could be given by the existence of one hysteretic component of the dissipation which is present in all tests.

2.4 Behavior for asymmetric and arbitrary loading

From the results of asymmetric loading tests it is possible to conclude that the loading or unloading paths followed by the material are independent on the preview strain history and only are function of the stress–strain state existing in the moment when the strain ratio is zero.

The response specimens subjected to seismic loadings shows the followings characteristics: in low strain levels (<30%) the rubber presents the most rigid response, for medium strain levels (50–150%) the average elastic modulus decrease respect to the low strain levels, but the area of the hysteretic cycles is increased. For high strain levels (>150%) hardening became noticeable, contributing to increase the stiffness.

3 Proposed model

The proposed model for the rubber strain–stress relationship has the following form:

$$F(x,\dot{x},t)=f_1(x,t)+f_2(x,t)=f(x,t)+c\dot{x}. \tag{1}$$

Where $F(x,v,t)$ is the total stress, x are the strain levels, t time, $\dot{x}$ the strain rate, f_1 the hysteretic component of the stress, f_2 is the viscous component and c is the equivalent viscous damping coefficient. Ref. [4].

F is a phenomenological description for the stress state in the material when is subjected to imposed displacement. The viscous component f_2 is taken equal to $0.12\dot{x}$, according to Ref. [4]. The expression for f_1 is given by Eq. (2).

$$f_1 = \underbrace{f_2\, d(x^{cv}, f_{NL}) + (f_1(x^{cv}) - f_2)}_{f_{11}} e + \underbrace{sgn(x) 5.0(\langle |x| - 1.5 \rangle)^{1.5}}_{f_{12}}. \tag{2}$$

Where f_{11} is the hysteretic nonlinear stress which is calculated solving the following system of differential equation (adapted from Computers and Structures for its software SAP200):

$$f_{11} = k_y(x^{cv}, f_{NL}^{cv})\, d(x^{cv}, f_{NL}^{cv}) + (k_e(x^{cv}, f_{NL}^{cv}) - k_y(x^{cv}, f_{NL}^{cv}))e. \tag{3}$$

$$\begin{aligned} &if\ \dot{d}e \geq 0 \quad \rightarrow \quad \dot{e}=(1-\left|\frac{e}{d_y(x^{cv}, f_{NL}^{cv})}\right|^{n(x^{cv}, f_{NL}^{cv})})\dot{d} \\ &else \quad \rightarrow \quad \dot{e}=\dot{d}. \end{aligned} \tag{4}$$

Being $K_e(x^{cv},f^{cv})$ and $K_y(x^{cv},f^{cv})$ the pre and post yielding stiffness, $d(x^{cv},f^{cv})$ the real strain of the system and e represents an internal variable of plastic strain which take a value in the range $[-d_y, d_y]$, (d_y is the yielding strain level). (x^{cv},f^{cv}) is the point in the strain-stress plane when $\dot{x}=0$. 'n' is the smoothing parameter for the zone between pre and post yielding branches in the hysteretic cycle. Fig. 3. The parameters K_e, K_y, d_y and n, are function of the point where the strain rate is zero.

The hardening is obtained by mean of adding an appropriated stiffer backbone to component f_{11}. For the present case the hardening function is the component f_{22} of Eq. (2).

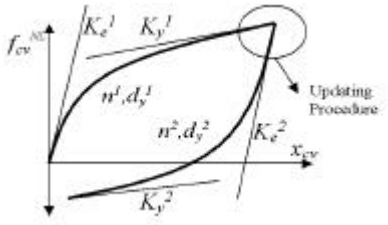

Figure 3: The upper curve is defined integrating the model for the initial parameters. When $\dot{x}=0$ parameters of the model are updated.

During the updating procedure it is necessary to have the model parameters expressed as function of the current stress and strain level. Therefore, it is necessary to estimate the functions f_1, f_2, f_3 and f_4, Eqs. (2) from experimental data.

3.1 Function f_1, f_2, f_3 and f_4

In this work an additional simplification will be made to construct the pre yielding stiffness function f_1, supposing that only is function of x^{cv}. A method for determining this function follows:

For each hysteretic cycle draw *the tangent line* to the point of the curve where $\dot{x}=0$. Construct the set of pairs composed by each *slope of the tangent line* and its corresponding *strain level*. Fit a polynomial to the set of the mentioned points. The obtained polynomial is the function f_1. The expression for f_1 is given in the Eq. (5).

$$f_1(x_{cv}) = -0.14 + 0.95x_{cv} - 2.45x_{cv}^2 + 3.19x_{cv}^3 - 2.25x_{cv}^4 + 0.89x_{cv}^5 - 0.20x_{cv}^6 + 0.04x_{cv}^7. \tag{5}$$

The post yielding stiffness f_2 is maintained constant and equal to the value of the slope of the upper enveloping curve Eq. (6).

$$f_2(x_{cv}, Fnl_{cv}) \approx K_y = 3.30. \tag{6}$$

The yield displacement function f_3 is constructed intersecting the line with slope f_1 and the enveloping

curve with slope f_2. The yield strain is measured from the zero strain level to the intersecting point. Eq. (7):

$$f_3(x_{cv}, Fnl_{cv}) \approx f_3(Fnl_{cv}) = \frac{|Fnl_{cv}| - |Fnl_0 - Fnl_{cv}|}{(f_2 - f_1)}. \qquad (7)$$

where Fnl_{cv} is the point where the strain rate is zero and Fnl_0 is calculated evaluating the straight line with slope f_2 at zero strain level.

After an optimization procedure the value of one was found for the smoothing function f_4. Eq. (8).

$$f_4(x_{cv}, Fnl_{cv}) \approx f_4 = 1.0. \qquad (8)$$

4 Comparison between numerical and experimental parts

The calibrated model was subjected to a sinusoidal record of imposed displacements with amplitude in the range [0.0-2.0] and loading frequency of 0.5 Hz. Fig. 4. Additionally, to the value of 0.12 Kg/s for the damping coefficient, two other fictitious values, (0.00 and 0.30), where employed to compare its influence in the response. From Fig. 4. it is possible to see that energy dissipation increase as viscous damping coefficient increase. The model is able to simulate energy dissipation for cuasi static loading, variable stiffness, and hardening for strain levels over 150%.

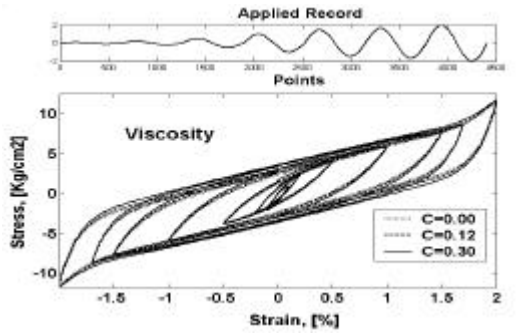

Figure 4: Upper: Imposed displacements record. Lower: Hysteretic cycles obtained for three values of damping coefficient.

The response model was compared with the experimental data for symmetric tests carried out with loading frequency of 0.5 Hz. Fig. 5. A good agreement is obtained for all strain levels but better fittings are obtained for strain levels over 50 %.

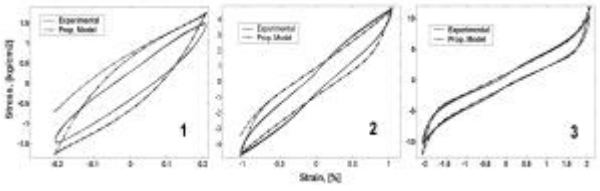

Figure 5: Predicted response and experimental data for symmetric sinusoidal tests, 0.5 Hz. Maximum strain levels: 1: 20 %, 2: 100 %, 3: 200 %.

Fig. 6 shows the rubber response for the seismic loading case. A good agreement between the predicted stress time history and the experimental data is obtained. (error: +/- 5 %).

Figure 6: Stress time history. Comparison between numerical simulation and experimental data.

5 Conclusions

The mechanical characteristic of a high damping rubber was studied in this work. Sets of tests were carried out for knowing the rubber response subjected to imposed displacements. The dependency of the response with frequency and strain level was studied. Among the more remarkable characteristics of the hysteresis are: strongly variable elastic stiffness and axial hardening for strain levels over 150 %. Additionally, a new model for the rubber behavior was proposed. The new model is constructed adding three components: a linear viscous dashpot acting in parallel with a stiffener backbone and a nonlinear hysteretic spring. All the parameters for the components of the proposed model have to be calibrated from experimental data. The model is validated comparing the predicted response with the data obtained from symmetrical and arbitrary tests.

Acknowledgment

This work has been partially supported by: The University of Chile, Project FONDECYT nº 1970732 and The Science and Tech. Ministry of Spain. Contract nº: BIA2003 – 08700 – C03 – 02.

References

[1] T.T. Soong, G.F. Dargush. *Passive Energy Dissipation System in Structural Engineering*. 1997.

[2] A. Chopra. *Dynamics of Structures: Theory and Applications to Earthquake Engineering (2nd Edition)*. Pearson Education; 2 edition (Sept. 2000).

[3] J.S. Hwang, S. W. Ku. Analytical modelling of high damping rubber bearings. *Journal of Structural Engineering*, Vol. 123. Nº 8. August 1997.

[4] P. Mata, R. Boroschek. Caracterización Mecánica de Goma de Alto Amortiguamiento para el Desarrollo de Disipadores de Energía. *2º Congreso iberoamericano de ingeniería sísmica.* Madrid 16-19 de Octubre de 2001.

[5] H. Kojima y Y. Yoshihide. Performance, Durability of High Damping Rubber Bearings for Earthquake Protection. *Rubber World*, Vol. 202, nº 4. (1990).